Quantum Cascade Structures under high magnetic field

Nicolas Péré-Laperne, Louis-Anne de Vaulchier, Yves Guldner, Carlo Sirtori, Vincent Berger

International Journal of Modern Physics B

QUANTUM CASCADE NANOSTRUCTURES UNDER HIGH MAGNETIC FIELD

N. PÉRÉ-LAPERNE,* L. A. DE VAULCHIER, Y. GULDNER
Laboratoire Pierre Aigrain, CNRS, Ecole Normale Supérieure,
24 rue Lhomond, 75005 PARIS, France
**nicolas.pere-laperne@lpa.ens.fr*

C. SIRTORI, V. BERGER
Laboratoire Matériaux et Phénomènes Quantiques, CNRS, Université Denis Diderot Paris 7,
Batiment Condorcet, 75205 Paris Cedex 13, France

Received 23 July 2008

Magneto-transport measurements have been performed on two quantum cascade structures, a laser and a detector. These experiments lead to determine the different scattering processes involved in these devices. In the lasers we find both an interface roughness mechanism and LO-phonon scattering of hot carriers in the upper state's Landau levels. In detectors we discover that an inelastic mechanism increase the dark current whereas an elastic one limits the detectivity.

Keywords: Heterostructures; quantum cascade; mid infrared; magneto-transport.

1. Introduction

In the last decade a variety of quantum cascade structures has been developed among them the popular Quantum Cascade Laser[1] (QCL). First developed in the infrared (IR) range, the structure has been modified to reach the THz one.[2] Recently, Quantum Cascade Detector (QCD) has been proposed as a new type of infrared photovoltaic detector[3] working without any applied bias and has been also extended to the THz range.[4] In a semiconductor quantum wells (QWs) structure, magnetic field applied along growth direction breaks the 2D in-plane continuum into discrete Landau levels (LLs). Thanks to the quantization, we can study the different processes involved in the scattering of electrons.[5,6] First, in a THz QCL in which the extraction miniband is coupled to a LO-phonon stage,[7] we perform magneto optical measurements and put in evidence a high electronic temperature population on the upper laser state.[8] Then magneto-transport measurements in QCDs allow us to identify the intricate scattering mechanisms responsible for the different transitions in the QCD with and without illumination. Doing so we are able to study respectively the dark current and an unforseen scattering process involving ionized impurities.

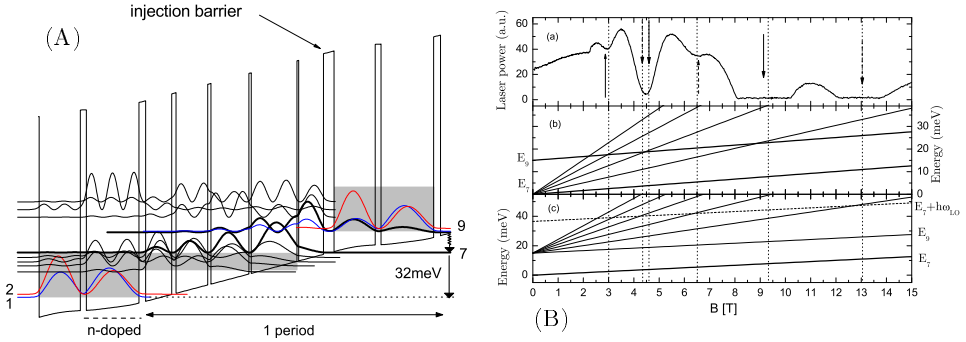

Fig. 1. (A) Self-consistent solution of coupled Schrodinger and Poisson's equations for one period of the structure. Layer sequence is given in Ref. 8. (B) (a) Emitted power as a function of the magnetic field under a constant current $J = 236\,\mathrm{A.cm^{-2}}$. (b) and (c) Fan charts of the laser LLs. Note in (b) the crossing at 9, 4.5 and 3 T; and in (c) the crossing at 13, 6.5 and 4.3 T.

2. Study of a THz QCL

The QCL active region is a GaAs/$Al_{0.15}Ga_{0.85}As$ sequence.[7] Fig. 1(A) shows the band diagram of one period of the active region under an electric field of 4 kV/cm. The radiative transition occurs between levels $|9\rangle$ and $|7\rangle$ ($E_{97} = 15\,\mathrm{meV}$). Lasers are mounted at the center of a superconducting coil where a magnetic field B up to 15 T can be applied parallel to the growth axis. The laser beam is focused onto a silicon bolometer below the device. The output power P as a function of B at $T = 2\,\mathrm{K}$ is shown in Fig. 1(B-a). A first series of minima (solid arrows) is observed for magnetic field values such that $E_{97} = n\hbar\omega_c$, where n is an integer. When this condition is fulfilled, an additional relaxation path opens for electrons in the LL $|9,0\rangle$ to elastically scatter into the LLs $|7,n\rangle$. This leads to a strong decrease of the population inversion between $|9,0\rangle$ and $|7,0\rangle$ and hence of the output power P. Fig. 1(B-b) shows $|9,0\rangle$ and $|7,n\rangle$ as functions of B. We observe that minima of P correspond to the crossing between LLs. From Fig. 1(A) we can see that the relevant wavefunctions are delocalized over several QWs and we believe that the relevant elastic scattering process is essentially the interface roughness.[6] In particular, the laser switches off between 8 and 10 T due to the fundamental elastic resonance ($E_{90} = E_{71}$). From the comparison between Figs. 1(B-a) and 1(B-b), we can see that the minimum at 6.5 T cannot be ascribed to the elastic scattering process described before. Furthermore, we observe that the laser switches off between 12 and 14 T, after the fundamental elastic resonance. Fig. 1(B-c) shows the excited LLs of $|9\rangle$, as well as the fundamental ones of $|7\rangle$. The dashed line indicates the first LO-phonon replica of $|7,0\rangle$. We notice that at 13 T, $|9,1\rangle$ has a phonon resonance with $|7,0\rangle$: $E_{91} - E_{70} = \hbar\omega_{LO}$. We show that this relaxation mechanism is a result of hot electrons in the injector that decrease the gain in the structure.[8] After the fundamental elastic resonance at 9 T, the system is in the extreme quantum limit. In order to understand why the laser switches off at 13 T, we assume that the

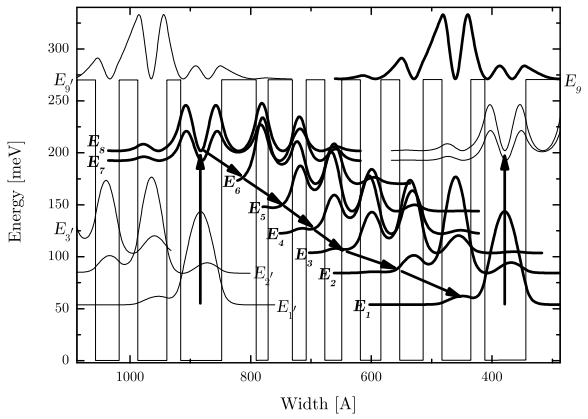

Fig. 2. Conduction band diagram of one period of an 8 μm QCD showing the energy levels. Note that the ground state of the first QW belongs to the former period and is noted $E_{1'}$. The arrows illustrate the electronic path during a detection event. The layer sequence is given in Ref. 9. The n-doping of the large QW is $5 \times 10^{11}\,\mathrm{cm}^{-2}$.

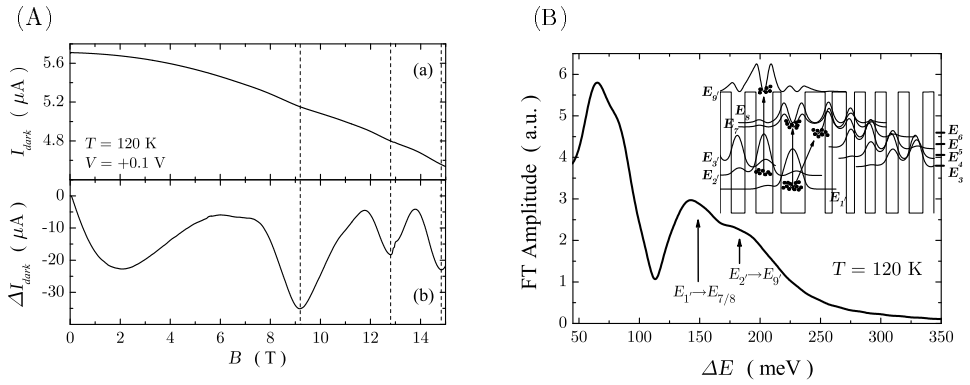

Fig. 3. (A) (a) Dark current as a function of B. (b) Same curve where the continuous contribution has been subtracted. (B) Fourier Transform amplitude of experimental ΔI_{dark} vs ΔE (see text).

electronic temperature T_e in the injector is greater than the lattice temperature T_l ($T_e = T_l + 150\,\mathrm{K}$) in order to fill the excited LLs of upper laser state.

3. Study of a mid-IR QCD

The QCD under study is a $GaAs/Al_{0.34}Ga_{0.66}As$ structure with a detection wavelength of 8 μm[9] (see Fig. 2). QCDs are mounted at the center of a superconducting coil where a magnetic field up to 17 T is applied parallel to the growth axis.

3.1. *Dark current analysis*

The so called dark current (current without illumination) is a limiting factor for the performance of detectors. In the case of QCDs, the dark current generally involves

several diagonal transitions from one cascade to the next. In order to reveal all these parallel contributions, magneto-transport measurements at $T = 120\,\mathrm{K}$ has been performed allowing a clear identification of the different electronic paths that contribute significantly to the dark current. The experiment consists of measuring I_{dark} along the device, kept under constant voltage ($V = 0.1\,\mathrm{V}$), while the magnetic field is swept up to its maximum value.[9] A typical result is illustrated in Fig 3(A-a). The dark current shows slight oscillations as a function of B, superposed on a general behavior corresponding approximately to a quadratic decrease. This line shape is removed from I_{dark} to give ΔI_{dark} shown in Fig 3(A-b). Then we perform a Fourier transform in order to extract the characteristic frequencies of each oscillation series and we plot it as a function of ΔE (through $\Delta E = \hbar eB/m^\star + \hbar\omega_{LO}$) as we assume that the transition is mediated by LO-phonon absorption.[9] The inset is a guide for the eye to identify the electronic transitions observed in these spectra. We observe both transitions $E_{1'} \rightarrow E_{7/8}$ and $E_{2'} \rightarrow E_{9'}$. We can see that a fair quantity of electrons are present on $|9'\rangle$ at high energy and explains an important leakage of electrons at high temperature. Therefore this particular point gives us a picture of the limiting factor of high temperature working condition.

3.2. *Experiments under illumination*

The working principle of QCDs under illumination without any applied voltage is the following. Electrons are excited from the ground level $E_{1'}$ to the upper level E_7 thanks to the light. Therefore a photocurrent is flowing through the structure and corresponds to the electrons going towards the cascade of levels. Light is emitted by a globar source from a FTIR spectrometer and guided to the sample. The experiment consists in measuring the current under illumination (i_{80K}) without any applied voltage while the magnetic field is swept to its maximum value. Results are illustrated in Fig 4(b). The photocurrent shows oscillations as a function of B, superposed on a general behavior corresponding approximately to a quadratic decrease. In order to remove this continuous component, we subtract the experimental data to a second order polynomial fit as shown on Fig 4(c). On the figure, minima of current are located at $B = 11.3$, 13.0 and 15.2 T. We propose a model of transport in one period by a rate equation approach and assume that electrons are in the upper detector state (E_7) through absorption of a photon. Current as a function of lifetimes involved in this structure can be written:

$$\frac{J}{q} = \alpha N_{1'}\left(\frac{\tau_{7-1'}}{\tau_{7-1'} + \tau_{7-c}}\right) = \alpha N_{1'} Q \tag{1}$$

where α and $N_{1'}$ are the absorption factor and population of $|1'\rangle$. The only figures which varies under magnetic field are the lifetimes, directly deducted from calculation of scattering rates of the different elastic and inelastic mechanisms. We present in Table 1 the lifetimes of the three scattering processes, LO-phonon emission, interface roughness and impurities scattering at $B = 0$. We observe that impurities scattering is the most efficient process. Indeed the wave function of $|7\rangle$ is localized

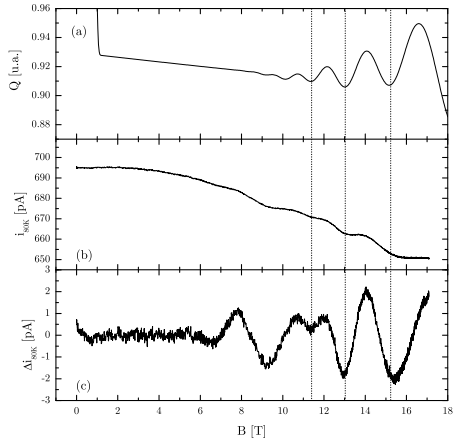

Table 1. Rate of different scattering processes for an electron on the 7 subband at $B = 0$.

Scattering mechanisms	$1/\tau_{7\text{-}1'}$ (s^{-1})	$1/\tau_{7\text{-}c}$ (s^{-1})
LO phonon	7.0×10^{11}	7.9×10^{11}
Interface roughness	2.0×10^{11}	2.5×10^{12}
Impurity scattering	3.5×10^{13}	4.5×10^{13}

Fig. 4. (a) Quantum efficiency as a function of B calculated from electronic lifetimes. (b) Current under illumination as a function of B at 80 K and 0 V. (c) Current under illumination as a function of B where the continuous contribution has been subtracted.

on the three first wells of the structure, and the doped well exactly corresponds to the active region. For the interface roughness, we used the parameters given in Ref. 6. Because we don't have access to impurities scattering rate as a function of B, we compare the oscillations on experimental data to calculation made versus B and involving another elastic process e.g. interface roughness (Fig. 4(a)). We observe that minima are all well reproduced. We conclude that the dominant scattering process is an elastic one and owing to zero magnetic field consideration, impurities scattering process is assumed to be the dominant one.

4. Conclusion

We have investigated the output power dependence under applied magnetic field of a QCL. Two distinct series of oscillations are identified corresponding to first, an elastic scattering from the fundamental LL of the upper subband and second, the relaxation of hot electrons via LO-phonon emission. In QCD, we put in evidence the different paths of leakage without illumination. Under illumination, we observe oscillations of current as a function of B. These oscillations are due to the modulation of the scattering rate of an elastic process.

References

1. J. Faist, F. Capasso, D. L. Sivco, C. Sirtori, A. L. Hutchinson, and A. Y. Cho, *Science* **264**, 553 (1994).
2. R. Kohler, A. Tredicucci, F. Beltram, H. E. Beere, E. H. Linfield, A. G. Davies, D. A. Rithcie, R. C. Iotti, and F. Rossi, *Nature* **417**, 156 (2002).
3. L. Gendron, M. Carras, A. Huynh, V. Ortiz, C. Koeniguer, and V. Berger, *App. Phys. Lett.* **85**, 2824 (2004).

4. M. Graf, G. Scalari, D. Hofstetter, J. Faist, H. Beere, E. Linfield, D. Ritchie, and, G. Davies, *App. Phys. Lett.* **84**, 475 (2004).
5. D. Smirnov, C. Becker, O. Drachenko, V. V. Rylkov, H. Page, J. Leotin, and C. Sirtori, *Phys. Rev. B* **66**, 121305(R) (2002).
6. A. Leuliet, A. Vasanelli, A. Wade, G. Fedorov, D. Smirnov, G. Bastard, and C. Sirtori, *Phys. Rev. B* **73**, 085311 (2006).
7. G. Scalari, N. Hoyler, M. Giovannini, J. Faist, *Appl. Phys. Lett.* **86**, 181101 (2005).
8. N. Péré-Laperne, L. A. de Vaulchier, Y. Guldner, G. Bastard, G. Scalari, M. Giovannini, J. Faist, A. Vasanelli, S. Dhillon and C. Sirtori, *Appl. Phys. Lett.* **91**, 062102 (2007).
9. A. Gomez, N. Péré-Laperne, L. A. de Vaulchier, C. Koeniguer, A. Vasanelli, A. Nedelcu, X. Marcadet, Y. Guldner and V. Berger, *Phys. Rev. B* **77**, 085307 (2008).